Representing Volumetric Vascular Structures Using Curve Skeletons*

Ingela Nyström
Centre for Image Analysis
Uppsala University
Lägerhyddsvägen 17
SE-75237 Uppsala
SWEDEN
ingela@cb.uu.se

Gabriella Sanniti di Baja
Istituto di Cibernetica
Italian National Research Council
Via Toiano 6
IT-80072 Arco Felice (Naples)
ITALY
gsdb@imagm.cib.na.cnr.it

Stina Svensson
Centre for Image Analysis
Swedish Univ. of Agric. Sc.
Lägerhyddsvägen 17
SE-75237 Uppsala
SWEDEN
stina@cb.uu.se

Abstract

This paper describes a technique to represent relevant information of tree-like structures in a compact way. The technique is general. In the application described here, the images are obtained with contrast-enhanced magnetic resonance angiography (MRA). After segmentation, the vessels are reduced to fully reversible surface skeletons. Thereafter, a novel approach to curve skeletonization based on the detection of junctions and curves in the surface skeleton is used. This procedure results in a good description of the tree structure of the vessels, where they are represented with a much smaller number of voxels. This representation is suitable for further quantitative analysis, e.g., measurements of vessel width and length.

1 Introduction

Skeletonization is a process where objects are reduced to structures of lower dimension while preserving topological properties as well as the general shape of the object. Some algorithms produce surface skeletons, some reduce the objects to curve skeletons. Thin elongated objects, such as blood vessels, are well suited for reduction to curve skeletons.

Volume (3D) images of the vascular system can be obtained from, e.g., magnetic resonance angiography (MRA) [1, 12]. Volume imaging usually implies large amounts of data, and it is, in general, a non-trivial problem how to present these volumes. Despite the large data volumes, the relevant information in an MRA data set is rather limited. Usually, the diagnostic physician is interested in the vessel anatomy, i.e., in the tree structure of the vessels, and in variations in vessel width. If the vessels can be identified using their branching points and the possible stenoses, or narrow parts, this is usually an adequate description of the vessel system. In this paper, we present a method to use a curve skeleton to extract this important information from a volume image of the vascular system.

There are previous works with the aim to obtain curve skeletons for medical applications. In [7], the application is visual analysis of computed tomography (CT) lung data. In [5], the skeleton concept from [6] is adopted, for use in interactive virtual colonoscopy rendered from spiral CT scans. Another example is [18], where, e.g., the curves are used in a tool for visualization of structures extracted from magnetic resonance imaging (MRI) brain data.

We borrow the underlying ideas from the method presented in [9]. The main differences are the introduction of an intermediate step aimed at simplify the structure of the surface skeleton and the use of a new curve skeletonization algorithm that performs significantly better. We compute fully reversible, distance-based surface skeletons, that are further reduced to curve skeletons using classification of the voxels of the surface skeleton. The theoretical concepts of the skeletonization algorithms are outlined in Section 2. The image processing operations used in the MRA application are described in Section 3 together with preliminary results.

2 Skeletonization

We are interested in the reduction of a solid object to a curve skeleton, via the surface skeleton. This is performed in four major steps, described in this section. The first step is a surface skeletonization algorithm. We have chosen the algorithm introduced in [15]. The three remaining steps are surface simplification, curve skeletonization, and, finally, thinning to curve skeletons of one-voxel thickness. These three steps can be applied to any surface skeleton, including two-voxel thick surface skeletons.

2.1 Notions

We assume binary volume images have been obtained, e.g., by segmenting a grey-level image into solid objects and background. We use a segmentation based on fuzzy connectedness, [16]. The 26-connectedness is chosen for the objects and, thus, the 6-connectedness for the background.

In a *distance transform (DT)* [2], each object voxel is labelled with the distance to its closest background voxel. Here, we have chosen the simplest distance for volume images, D^6, which is the 3D equivalent of the city-block distance. The D^6 distance between two voxels is the number of steps in a minimal 6-connected path between the voxels. The DT is computed by a forward and a backward scan over the image, propagating distance information and accordingly labelling with increasing value for more internal voxels. We denote the DT based on the D^6 distance DT^6.

The distance label of a voxel v in the DT can be interpreted as the radius of a digital ball centred on v. An object voxel is called a *centre of a maximal ball* (CMB), if the associated ball is not completely covered by any other single ball in the object. For DT^6, the CMBs are equivalent to the local maxima, i.e., voxels having no face-neighbour with higher label. The union of the maximal balls, which may be computed by applying the *reverse* D^6 *distance transformation* to the set of CMBs, coincides with the object. Hence, the set of CMBs is a compact representation of the object.

2.2 Surface skeletonization by direct identification on DT^6

The surface skeletonization algorithm used, [15], directly identifies and marks the skeletal voxels on DT^6 in a number of scans. The voxels in the neighbourhood of the current voxel are interpreted differently depending on their distance values and whether they are already marked or not. By this, iterative thinning is simulated. As soon as no new skeletal voxels are marked during a scan, the process terminates and the surface skeleton is detected. The number of scans is independent of the thickness of the object, which is not the case when iterative thinning is used. This is of importance, especially for thick objects. Typically the number of scans needed is between 8 and 16, depending on the complexity of the topology of the object.

The resulting surface skeleton is centred within the object (with respect to the D^6 distance), almost symmetric, fully reversible (since the set of CMBs is included), topologically equivalent to the original object, and partly two-voxel thick. By having an almost symmetric surface skeleton, further analysis will be improved, e.g., a more symmetric curve skeleton may be obtained.

2.3 Surface skeleton simplification

The surface skeleton can be simplified by removing short curves (one- and two-voxel thick) in the border of the surface skeleton. Only curves corresponding to minor features of the object should be removed. We use the simplification algorithm introduced in [4]. There, distance information is used to distinguish short curves, whose voxels are possibly deleted. Remaining more significant curves are untouched.

During simplification, the border of the surface skeleton, which consists of both curve and edge voxels, is detected using the classification in [14]. The voxels in the curves closest to the remaining part of the surface are marked. From these a "removal" marker is propagated in a number of steps (chosen by the user). If a curve is completely marked it is removed, unless topology is changed.

2.4 Curve skeletonization by junction detection

The curve skeletonization algorithm [10] is based on iterative thinning and on the detection of junctions and curves in the surface skeleton. The different classes of voxels in the surface skeleton we are interested in are *junction*, *inner*, *edge*, and *curve* voxels, see Figure 1. Voxels in surfaces of one-voxel thickness can be classified into these classes by investigation of their $3 \times 3 \times 3$ neighbourhood [8, 13]. However, complex cases where surfaces are crossing each other would not produce a consistent classification at junctions, e.g., when shifting one of the crossing surfaces one voxel (Figure 2). Moreover, surface skeletons of objects having regions with even thickness are not properly handled. We use the classification described in [14], which handles both one- and two-voxel thick surface skeletons.

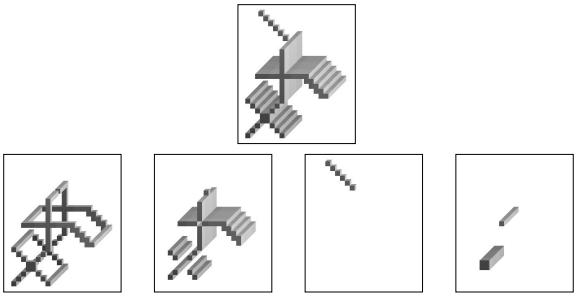

Figure 1. A surface (top) with its classification (bottom).

The curve skeleton is obtained in two steps, both being iterative. Each iteration of both steps includes two subiterations: 1) detection of edge voxels, and 2) voxel removal by means of topology preserving removal operations. The two

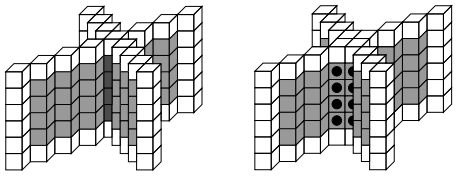

Figure 2. Edge voxels (white), inner voxels (grey), and junction voxels (dark grey) according to [8, 13]. Voxels with • should be classified as junction voxels for consistency.

steps differ in the selection of the voxels that, at each iteration, are checked to identify the edge voxels, i.e., the set of voxels candidate for removal. In the first step, only voxels *initially* (i.e., on the original surface skeleton) classified as inner (or edge) voxels are checked during the identification of the edge voxels. Note that we do not need any end-point detection criterion, because during the first step (curve and) junction voxels are not checked to establish whether they have become edge voxels, iteration after iteration. In the second step, also voxels initially classified as junction voxels are checked during the identification of the edge voxels. Edge voxels that have been transformed into curves during the first step are not interpreted as edge voxels and, hence, are automatically preserved. In both steps, standard topology preserving removal operations are sequentially applied on the current set of edge voxels. See [10] for details.

A box of size $60 \times 40 \times 20$ voxels and its D^6 surface skeleton are shown in Figures 3(a) and (b). The skeletal set resulting after the first step is shown in Figure 3(c). Voxels detected as junction voxels during the initial classification are partly transformed into curve voxels, and partly into edge voxels surrounding the rectangular surface (two-voxel thick) found in the middle of the box. The curve skeleton (two-voxel thick in the central part) is the set resulting after the second step, see Figure 3(d).

2.5 Final thinning

The curve skeleton can be further reduced to one-voxel thickness. This is performed in two steps using the final thinning from [3]. During the first step, voxels in the curve skeleton that were classified as curve or junction voxels in the surface skeleton are not considered for removal as they are playing a more important role than voxels ascribed to the curve skeleton only for connectedness preservation. During the second step, all voxels in the curve skeleton are considered. The final thinning is achieved by identifying tip-of-protrusions and iterative removal of voxels using standard topology preserving operations. The extra cost due to the two steps used for the final thinning is repaid by a more significant curve skeleton.

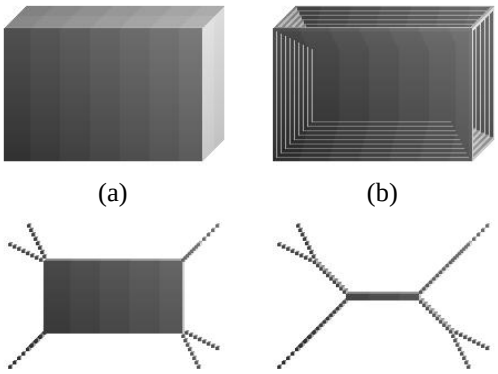

Figure 3. A box (a) with its D^6 surface skeleton (b). The intermediate result (c) and the final result (d) of the curve skeletonization.

3 Application — Skeletonization in MRA

Magnetic resonance angiography (MRA) is a set of magnetic resonance imaging (MRI) techniques to non-invasively imaging the flow of blood in vessels [1, 12]. The technique used in this study is Gadolinium (Gd) contrast-enhanced angiography, which does not rely on flow effects, but on the effect that Gd has on the MR signal, given as an intravenous injection. The Gd-MRA image acquired is a thoracic data set of a patient. The $512 \times 512 \times 47$ image was obtained with a 1.5 T magnet (Philips Gyroscan ACS-NT). The voxel size was $0.97 \times 0.97 \times 2.5$ mm^3. Figure 4 (left) presents a part of the volume as a maximum intensity projection (MIP), the commonly used projection method for such images. The vessel system is shown clearly, but without depth information.

When applying skeletonization in the analysis of the blood vessels in the image described above, the following image processing operations were performed:

1. **Interpolating the image to cubic voxels.** Distance computations and connectivity aspects are simpler if distances between layers are the same in all x, y, z-directions. Therefore, the anisotropy of the image is eliminated by a linear interpolation of the image to cubic voxels. There exist other (not as simple) solutions to this problem. In this particular case the resampled image is of size $500 \times 500 \times 125$. Due to the artifacts in the lower part of the image, we have selected the area indicated by the white square in Figure 4 (left), resulting in a $256 \times 256 \times 125$ image, i.e., 8 Mbytes.

2. **Segmentation of the blood vessels.** The segmentation is performed using fuzzy connectedness. Voxels that

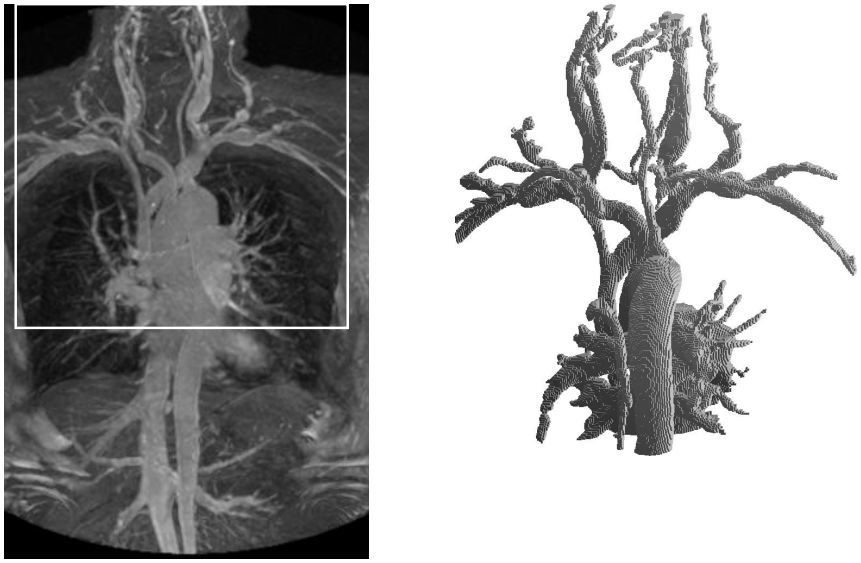

Figure 4. MIP of the MRA image (left). Rendered 2D projection of the segmented vessels (right).

have high "hanging-togetherness" with a set of predefined seed voxels are segmented from the data set. See Figure 4 (right) for result from the segmentation into object and background. Segmentation is an important and difficult task. If a correct segmentation is not obtained, the results may be completely misleading. In many different applications, the concept of fuzzy connectedness [17] has been used with good results.

3. **Surface skeletonization.** The distance transform of the binary image is computed, in which every object voxel is given a label with the D^6 distance to its closest background voxel. On DT^6, the surface skeleton is detected as described in Section 2.2. The resulting surface skeleton is shown in Figure 5 (top-left). Note that the surface skeleton is two-voxel thick at parts where the original object had an even thickness. Complete recovery of the original object is possible from the distance labels, e.g., by the reverse distance transformation, since the complete set of CMBs is included at this stage.

4. **Surface skeleton simplification.** When we apply the surface skeletonization to real images, sensitivity to noise in the input data is revealed. Typically, the surface skeleton will have short curves in the surface border corresponding to "unsmoothness" in the original object. We use the simplification algorithm described in Section 2.3. The simplified surface skeleton is shown in Figure 5 (top-right), where curves of a maximal length of 3 voxels have been removed.

5. **Curve skeletonization.** The curve skeleton includes voxels placed in curves and peripheral junctions in the surface skeleton and voxels needed for topology preservation as described in Section 2.4. The resulting curve skeleton is shown in Figure 5 (bottom-left).

6. **Final thinning.** The curve skeleton is reduced to one-voxel thickness. This is performed as described in Section 2.5. See Figure 5 (bottom-right) for final result.

Another possibility compared to Step 1-6 could be to apply curve skeletonization to an already one-voxel thick surface skeleton as in [3, 9]. However, we have found that if reduction to one-voxel thickness is postponed until the curve skeleton has been obtained, and hence keeping the medial symmetry as long as possible, the risk of creating spurious branches in the curve skeleton is significantly reduced. This is now possible, since the curve skeletonization algorithm [10] can be applied also to two-voxel thick surface skeletons. Besides, even if the surface skeleton is reduced to one-voxel thickness, the obtained curve skeleton could still be two-voxel thick and would hence need final thinning anyway.

Another improvement in the process compared to [9] is the introduction of the simplification algorithm. By first simplifying the surface skeleton, the resulting curve skeleton gets a simpler structure, i.e., fewer branches, than if the curve skeleton is obtained from the non-simplified set.

By using these improved skeletonization steps, the final result shows a better representation of the vessels and branches than the algorithms presented in [9].

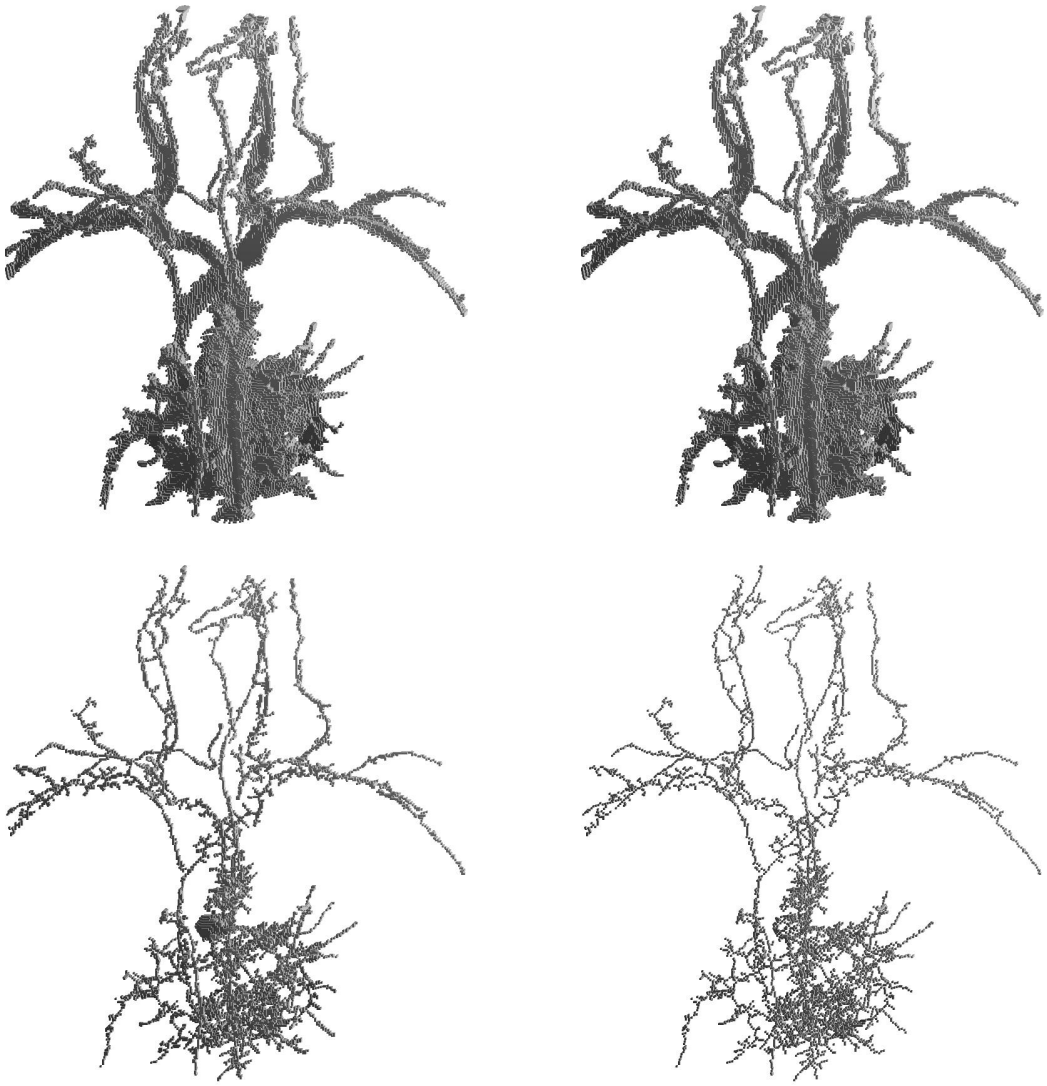

Figure 5. The surface skeleton and the simplified surface skeleton (top). The curve skeleton before and after final thinning (bottom).

All the skeletal representations give a significant reduction in number of voxels. The number of voxels in the surface skeleton is approximately 16% of the number of voxels in the original object (more than 330.000 voxels), whereas the final curve skeleton contains less than 2.2% of the original voxels, but still gives an impression of the general shape of the vessel tree. See Table 1 for details and for the CPU times for skeletonization of the MRA image in Figure 5 on a DEC Alpha workstation. The computational cost can be considered high only for the curve skeletonization algorithm. This is due to the (presently non-optimized) classification process that has to be repeatedly used during curve skeletonization.

4 Conclusion

We reduce a solid object to a curve skeleton via the surface skeleton. The use of such a medial representation of the vascular tree shows more clearly the geometrical properties of the blood vessels. In this paper, we have chosen to verify our curve skeletonization algorithm on the vessel structure in the thorax. Despite the choice of a complex structure, we have obtained promising results.

The jaggedness of the surface skeletons is either resulting from noise or from significant variations in the original object, in this case the vessels. In other words, one might risk to destroy clinically relevant information by simplify-

Table 1. Computational cost and number of voxels for the different representations.

	CPU time (in minutes)	# of voxels	%
Original object		335694	
Surface skeleton	1.25	55682	16.59
Simplified surface skeleton	1.75	52506	15.64
Curve skeleton	11	14432	4.30
Thinned curve skeleton	1	7480	2.23
Total time	**appr. 15**		

ing the surface skeleton. In the simplification algorithm in [4] this is controlled as much as possible by allowing only short curves to be removed (provided topology is not altered). Other more significant parts are left untouched.

The distance labels of the voxels in the curve skeletons give an indication of the *minimum* distance to the original background at that point. Further analysis of these values for vessel diameter measurements have already been found of interest [11]. Length measurements of vessels are also possible by path-following in the curve skeletons. The curve skeletons may, hence, be useful in quantitative shape analysis of the vessels.

Acknowledgement

We are thankful to Xavier Tizon for providing us with the segmented MRA image. Prof. Gunilla Borgefors, Centre for Image Analysis, Uppsala, Sweden, is also acknowledged for useful discussions on skeletonization.

References

[1] C. M. Anderson, R. R. Edelman, and P. A. Turski. *Clinical Magnetic Resonance Angiography*. Lippincott-Raven Publishers, New York, 1993.

[2] G. Borgefors. On digital distance transforms in three dimensions. *Computer Vision and Image Understanding*, 64(3):368–376, Nov. 1996.

[3] G. Borgefors, I. Nyström, and G. Sanniti di Baja. Computing skeletons in three dimensions. *Pattern Recognition*, 32(7):1225–1236, 1999.

[4] G. Borgefors, I. Nyström, G. Sanniti di Baja, and S. Svensson. Simplification of 3D skeletons using distance information. In L. J. Latecki, R. A. Melter, D. M. Mount, and A. Y. Wu, editors, *Vision Geometry IX*, pages 300–309. Proc. SPIE 4117, 2000.

[5] Y. Ge, D. R. Stelts, and D. J. Vining. 3D skeleton for virtual colonoscopy. In K. H. Höhne and R. Kikinis, editors, *Proceedings of* 4^{th} *VBC'96: Visualization in Biomedical Computing*, Lecture Notes in Computer Science, pages 449–454. Springer-Verlag, Berlin Heidelberg, 1996.

[6] T.-C. Lee, R. L. Kashyap, and C.-N. Chu. Building skeleton models via 3-D medial surface/axis thinning algorithms. *CVGIP: Graphical Models and Image Processing*, 56(6):462–478, 1994.

[7] C. M. Ma and M. Sonka. A fully parallel 3D thinning algorithm and its applications. *Computer Vision and Image Understanding*, 64(3):420–433, Nov. 1996.

[8] G. Malandain, G. Bertrand, and N. Ayache. Topological segmentation of discrete surfaces. *International Journal of Computer Vision*, 10(2):183–197, 1993.

[9] I. Nyström. Skeletonization applied to magnetic resonance angiography images. In K. M. Hanson, editor, *Medical Imaging 1998: Image Processing*, pages 693–701. Proc. SPIE 3338, 1998.

[10] I. Nyström, G. Sanniti di Baja, and S. Svensson. Curve skeletonization by junction detection. In C. Arcelli, L. P. Cordella, and G. Sanniti di Baja, editors, *Visual Form 2001*, volume 2059 of *Lecture Notes in Computer Science*, pages 229–238. Springer-Verlag, 2001.

[11] I. Nyström and Ö. Smedby. A new presentation method for magnetic resonance angiography images based on skeletonization. In S. K. Mun, editor, *Medical Imaging 2000: Image Display and Visualization*, pages 515–522. Proc. SPIE 3976, 2000.

[12] M. R. Prince. Gadolinium-enhanced MR aortography. *Radiology*, 191:155–164, 1994.

[13] P. K. Saha and B. B. Chaudhuri. Detection of 3-D simple points for topology preserving transformations with application to thinning. *IEEE Transactions on Pattern Analysis and Machine Intelligence*, 16(10):1028–1032, Oct. 1994.

[14] G. Sanniti di Baja and S. Svensson. Classification of two-voxel thick surfaces: a first approach. Internal Report 19, Centre for Image Analysis, 2000. Available from the authors.

[15] G. Sanniti di Baja and S. Svensson. Surface skeletons detected on the D^6 distance transform. In F. J. Ferri, J. M. Iñetsa, A. Amin, and P. Pudil, editors, *Proceedings of SSSPR 2000 - Alicante: Advances in Pattern Recognition*, volume 1876 of *Lecture Notes in Computer Science*, pages 387–396, Berlin Heidelberg, 2000. Springer-Verlag.

[16] X. Tizon and Ö. Smedby. Improving visualization of blood-pool agent MRA with virtual contrast injection. In *Proceedings of the ISMRM, 8th Scientific Meeting and Exhibition*, page 1535, Denver, CO, USA, 2000.

[17] J. K. Udupa and S. Samarasekera. Fuzzy connectedness and object definition: Theory, algorithms, and applications in image segmentation. *Graphical Models and Image Processing*, 58(3):246–261, May 1996.

[18] Y. Zhou, A. Kaufman, and A. W. Toga. Three-dimensional skeleton and centerline generation based on an approximate minimum distance field. *The Visual Computer*, 14(7):303–314, 1998.

This is a copy from E. Ardizzone and V. Di Gesù, editors, *Proceedings of* 11th International Conference on Image Analysis and Processing (ICIAP 2001), *Palermo, Italy*.